Published in final edited form as:
Proc IEEE Sens. 2017 ; 2017: .

Toward Sclera-Force-Based Robotic Assistance for Safe Micromanipulation in Vitreoretinal Surgery

Ankur Gupta[*], **Saurabh Singh**[*], **Berk Gonenc**, **Marin Kobilarov**, and **Iulian Iordachita**
Laboratory for Computational Sensing and Robotics, Johns Hopkins University, Baltimore, MD 21218, USA

Abstract

In vitreoretinal surgery instruments are inserted through the sclera to perform precise surgical maneuvers inside the eyeball, which exceeds typical human capabilities. Robotic assistance can enhance the skills of a novice surgeon, provide guidance during tool manipulation based on the desired behavior defined by expert surgeons' maneuvers, and consequently improve the surgical outcome. This paper presents an experimental study characterizing the safe/desired magnitude of forces between the surgical instrument and the sclera insertion port as a function of the tool insertion depth. We explore two types of regressions, a polynomial and a sum of sines fit, to describe the observed user behavior during our one-user pilot study, based on which a variable admittance control scheme can be implemented to robotically guide other users towards this desired behavior for a safe operation.

Keywords

fiber Bragg grating; force sensing; insertion depth sensing

I. Introduction

Retinal microsurgery demands advanced surgical skills such as excellent vision, depth perception, and fine motor control. These requirements exceed the fundamental physiological capability of many individuals. Inaccuracy in tool positioning (due to physiological hand tremor) and patient's movement are among the important factors limiting performance in vitreoretinal microsurgery. During vitreoretinal procedures, instruments are inserted into the eye through incisions on the sclera. After orienting the eyeball such that the surgical target on the retina is within the field of view of the operating microscope, the surgeon moves the surgical instruments to manipulate tissues by pivoting about the insertion port on the sclera. In this case, tool manipulation is confined to only three rotational degrees of freedom (DOF) about the sclerotomy and one translational DOF along the instrument axis. Application of excessive forces at the sclera contact can cause corneal striae and vision loss [1]. Continual monitoring of sclera forces can limit them at a safe level either by auditory feedback or via robotic assistance.

[*]Equal Contribution

In order to enhance the capabilities of microsurgeons, various robotic systems have been developed like master-slave teleoperated systems [2], handheld robotic devices [3], and untethered micro-robots [4]. We developed the Steady-Hand Eye Robot (SHER) (Fig. 1a) based on a hands-on cooperative variable admittance control where the surgeon and the robot together hold and move the surgical instrument [5,6]. This method damps the smaller forces conveyed by the hand tremor of the operator. It provides the desired precision and sensitivity of a robot as well as the manipulative transparency and immediacy of a hand-held instrument. Accompanying this improvement in tool manipulation precision, to detect the fine tool-to-tissue interaction forces in vitreoretinal surgery, we developed various force-sensing ophthalmic instruments based on fiber Bragg grating (FBG) sensors. Among these, our dual force-sensing tool [7] (Fig 1b) is capable of simultaneously measuring the force at the sclera contact, the tooltip forces and the tool insertion depth (Fig. 1c).

In robot-assisted retinal surgery, the stiffness of the robotic system attenuates the user's perception of the scleral forces while in freehand manipulation the surgeon can clearly sense these contact forces and guide the desired motion e.g., use the sclerotomy point as the tool's remote center-of-motion (RCM). This raises the risk of inducing potentially large and injurious sclera forces when using a robotic device. This study aims to identify the behavior of safe tool-sclera contact force variation as a function of tool insertion depth during routine manipulations in vitreoretinal surgery. The outcomes of this work will form the reference in designing a variable (linear and nonlinear) admittance control scheme for robotic guidance with enhanced safety as shown in Fig 2.

II. Control Algorithm

SHER normally operates under a variable admittance control scheme where the fundamental user input is the force applied on the instrument handle, which in turn controls the velocity by which the robot follows the user directed motion [8]. Current robot-assisted retinal surgery relies on the surgeon's fine motor skills, experience, and cognitive judgments. At the beginning of the operation, the surgeon orients the eyeball by translating the instruments inserted through the sclera and brings the surgical target into the field of view through the surgical microscope. During this phase, the tools are usually kept away from the delicate retina to avoid unintentional collisions, which means a small tool insertion depth varying within $[0, l_{lb}]$, where l_{lb} denotes the lower bound of insertion depth (Fig. 2). During this manipulation, the remote center of motion (RCM) constraints are not enforced; hence, the user has 6 degrees of freedom (DOF) to move the tool. After the orientation of the eyeball is adjusted, the tool is moved closer to the retina to interact with the surgical target, which corresponds to a tool insertion depth varying within $[l_{ub}, 25$ mm$]$, where l_{ub} is the upper bound of tool insertion depth, and 25 mm corresponds to the average human eyeball diameter. After this moment during the surgical maneuvers, the tool needs to be moved by pivoting about the insertion port on the sclera in order not to displace the eyeball. In other words, RCM constraints need to be obeyed allowing 4-DOF motion: rotations about 3 dimensions and axial insertion of the tool (Fig. 1c). Therefore, the desired tool manipulation behavior may change throughout the procedure depending upon the insertion depth, which can be measured by the dual force-sensing instrument and effectively used to update the robot admittance and adapt the appropriate behavior.

The equations of variable admittance control for SHER are [6]:

$$\dot{x}_{ss} = \alpha\left(\mathrm{A_{sh}F_{sh}} + \gamma \mathrm{A_{ss}F_{ss}}\right) \quad (1)$$

$$\mathrm{A_{sh}} = \mathrm{diag}([1-\beta, 1-\beta, 1, 1, 1, 1]^{\mathrm{T}}) \quad (2)$$

$$\mathrm{A_{ss}} = \mathrm{diag}([1+\beta, 1+\beta, 1, 1, 1, 1]^{\mathrm{T}}) \quad (3)$$

where $\dot{x}_{ss}$ is the desired velocity of the tool-sclera contact in sclera frame, F_{hh} and F_{hs} are the handle input force and the sclera contact force, A_{sh} and A_{ss} are the diagonal admittance matrices, and β ∈ [0, 1] is a scalar that can vary linearly or non-linearly along with the tool insertion depth as shown in Fig. 2. The admittance matrix A_{sh} removes the transverse force components. When the insertion depth is smaller than the given lower bound l_{lb}, we set β = 0 and $A_{sh} = A_{ss} = I$, which leads to the force scaling control mode providing 6-DOF freedom to reposition the eye with scaled sclera force feedback. When the insertion depth is larger than the given upper bound l_{ub}, we set β = 1, which switches the operation mode to enable virtual RCM constraints with doubled gain for minimizing the transverse forces at the tool-sclera contact.

The motivation for this study is to develop the non-linear transition function for β to control robot admittance (shown in red in Fig. 2) for the safe eye manipulation when the tool insertion depth is between $[l_{lb}, l_{ub}]$. The robot admittance control for $l_{lb} \le d \le l_{ub}$ can be designed by introducing $\beta = F_{desired}/F_{actual}$ for a particular tool insertion depth. Here, $F_{desired}$ is a function of tool insertion depth, which can be characterized experimentally by monitoring the tool-sclera contact force variation during routine manipulations inside the eye. F_{actual} is the intra-operatively detected tool-sclera force. This control law will drive the robot with a velocity that will bring the measured tool-sclera forces toward the desired level, which will vary depending on the tool insertion depth throughout the manipulation.

III. EXPERIMENTS

We designed an experiment to record forces at the tool-sclera contact during routine eye manipulation trying to reach several targets on the simulated retina surface of an artificial eyeball phantom. The experimental setup (Fig. 1a) consists of the SHER system, a dual force-sensing tool (Fig. 1b), an optical sensing interrogator (sm130–700 from Micron Optics Inc., Atlanta, GA), an artificial eye phantom (Fig. 3a), a digital microscope (USB2-Micro-200X, Plugable Technologies) and a computer system (Intel i7 processor with 8 GB RAM). The eyeball phantom was developed in our previous work [9]. For this experiment, we placed the artificial eyeball into a 3D printed socket and used mineral oil at the interface to provide lubrication and enable movement of the eyeball inside the socket with a realistic resistance. Inside the eyeball, 3 targets were marked on the retina surface at 30 degrees from the normal to the center of the eye using different colors (red, black, green) (Fig. 3b). To visualize the retina surface, the digital microscope was placed above the eye phantom and its output was displayed to the operator on a monitor. The Bragg wavelengths of FBGs on the force-sensing tool were acquired by the optical sensing interrogator and converted into force and insertion depth values following [7].

In order to indicate the center of the view through the microscope, a fixed mark was overlaid on the screen. Then, similar to the standard vitreoretinal surgery, we asked the operator to insert two instruments, a light pipe, and our dual force-sensing tool, into the eye phantom through the openings on the sclera and perform a set of manipulations. The task in the experiment consisted of two maneuvers. First was to adjust the orientation of the eyeball by moving the tools and to bring a surgical target (one of the green, red and black marks on the retina surface) onto the fixed central mark on the screen. The second maneuver was to approach the retina by inserting the force-sensing tool axially, to touch the target on the retina, and to retract the tool back to its initial position. This procedure was repeated for each target 10 times switching between the targets in random order. The insertion depth and the forces induced on the sclera contact during these manipulations were recorded.

IV. RESULTS

A sample depth and sclera force recording while approaching and touching two consecutive targets is shown in Fig. 4. Accordingly, the first target was touched after inserting the tool 19.9 mm deep into the eye while the second target was within the reach of the tool after 12.4 mm of insertion. After touching the initial target, the tool was first moved away from the retina and then moved laterally to reorient the eyeball and bring the second target onto the center of the camera view. During this period, the sclera forces varied up to 74.5 mN. Overall, the measured forces on the sclera were observed to be of larger amplitude with higher variance while reorienting the eyeball and remained relatively small with fewer changes while approaching the retinal targets.

To obtain the tool-sclera contact force variation, we computed the median of the sclera contact forces recorded for each mm of the measured insertion depth throughout all the trials, resulting in the scatter points shown in Fig 5. We explored two distinct fits, a polynomial regression, and a sinusoidal fit, to describe this data. After experimenting various orders, the closest fit that can be obtained without over-fitting in each category were a 4th order polynomial and a 3rd order sum of sines function as given by equations (4) and (5), respectively.

$$f(x) = p1 * x^4 + p2 * x^3 + p3 * x^2 + p4 * x + p5 \quad (4)$$

$$f(x) = a1 * \sin(b1 * x + c1) + a2 * \sin(b2 * x + c2) + a3 * \sin(b3 * x + c3) \quad (5)$$

The identified best fits are shown by the continuous blue dashed and red solid curves in Fig. 5, respectively. The root mean square of error (RMSE) of the polynomial fit (p1=−0.002, p2=0.12, p3=−2.193, p4=13.53, p5=5.46) was 4.70 mN (R^2=0.76) while the sinusoidal model (a1= 24.53, a2=10.82, a3=10.14, b1=0.06, b2=0.49, b3=0.64, c1=1.13, c2=−1.79, c3= −0.37) could more closely describe the variation with an RMSE of 4.25 mN (R^2=0.81).

V. Conclusion

This paper presented an experimental study to characterize the tool-sclera contact forces as a function of the tool insertion depth during vitreoretinal manipulations. The outcomes of this work form the initial steps toward the development of a variable admittance control scheme to provide safer robot-assisted eye manipulation. Results have demonstrated the feasibility of the proposed experimental procedure; nevertheless, the current data belongs to a single user that is not an expert surgeon. In our future work, we aim to repeat experiments with multiple vitreoretinal surgeons to better define the characteristics of expert and safe maneuvers during the key surgical tasks and design the control scheme of SHER to robotically guide novice users toward this pattern.

Acknowledgments

This work was supported by the National Institutes of Health under 1R01EB023943-01 and in part by Johns Hopkins University internal funds.

References

1. He, X. Ph D Thesis. Johns Hopkins University; Baltimore: Jul, 2015 Force Sensing Augmented Robotic Assistance for Retinal Microsurgery.
2. Tsirbas A, Mango C, Dutson E. Robotic ocular surgery. The British Journal of Ophthalmology. Jan; 2007 91(1):18–21. [PubMed: 17020903]
3. Riviere CN, Ang WT, Khosla PK. Toward active tremor canceling in handheld microsurgical instruments. IEEE Transactions on Robotics and Automation. 2003; 19(5):793–800.
4. Kummer MP, Member SS, Abbott JJ, Kratochvil BE, Borer R, Sengul A, Nelson BJ. OctoMag: An Electromagnetic System for 5-DOF Wireless Micromanipulation. IEEE Transactions on Robotics. 2010; 26(6):1006–1017.
5. Mitchell B, Koo J, Iordachita I, Kazanzides P, Kapoor A, Handa J, Hager G, Taylor R. Development and application of a new steady-hand manipulator for retinal surgery. IEEE International Conference on Robotics and Automation. 2007:623–629.
6. He X, Roppenecker D, Gierlach D, Balicki M, Olds K, Gehlbach P, Handa J, Taylor R, Iordachita I. Toward clinically applicable steady-hand eye robot for vitreoretinal surgery. ASME 2012 International Mechanical Engineering Congress and Exposition. :145–153.
7. He X, Balicki M, Gehlbach P, Handa J, Taylor R, Iordachita I. Multi-Function Force Sensing Instrument for Variable Admittance Robot Control in Retinal Microsurgery. IEEE International Conference on Robotics and Automation (ICRA). 2014
8. Okunev V, Nierhoff T, Hirche S. Human-preference-based control design: Adaptive robot admittance control for physical human-robot interaction. IEEE International Symposium on Robot and Human Interactive Communication IEEE. Sep.2012 :443–448.
9. Gupta A, Gonenc B, Balicki M, Olds K, Handa J, Gehlbach P, Taylor RH, Iordachita I. Human Eye Phantom for Developing Computer and Robot-Assisted Epiretinal Membrane Peeling. Proc International Conference of the IEEE EMBS (EMBC'14). 2014:6864–6867.

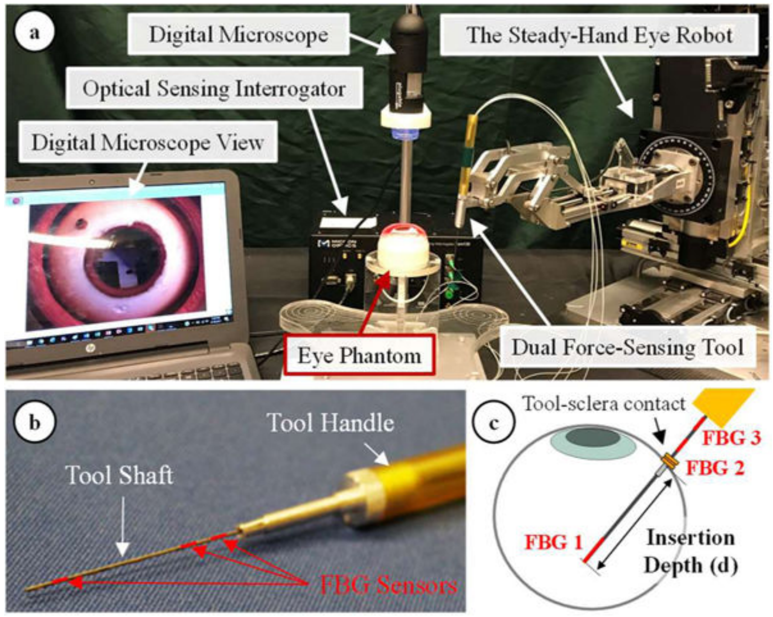

Figure 1.
(a) Experimental setup. (b) Dual force-sensing tool with FBG sensors (shown in red) that measures both tool tip force and the forces at the sclera contact [7]. (c) 3 FBGs located along the tool shaft provide insertion depth and the force at the tool-sclera contact.

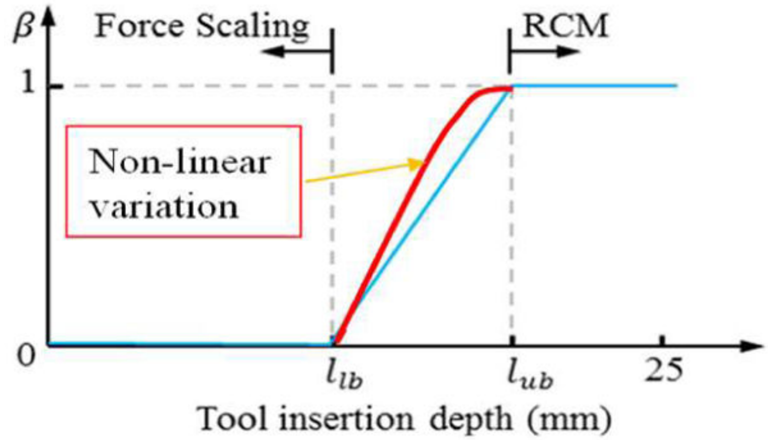

Figure 2.

Admittance modulation (linear or non-linear) along the insertion depth. The section between l_{lb} and l_{ub} is the transition between pure force scaling of the sclera force and pure RCM behaviors.

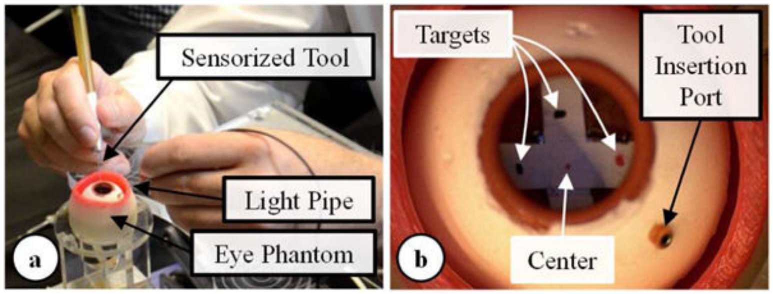

Figure 3.

(a) User performing manipulations with the sensorized tool inside the phantom eye. (b) Top view of the eye phantom with 3 targets marked in different colors (red, black, green) on the retina surface.

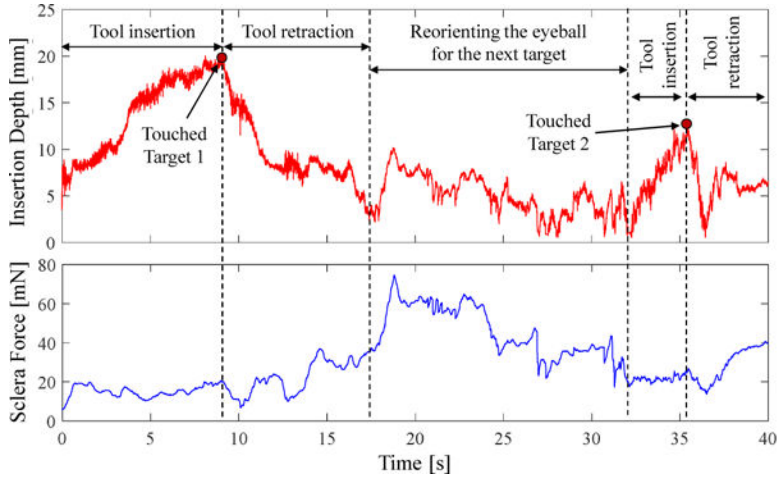

Figure 4.
Tool insertion depth and sclera contact force measurements from a representative trial while approaching and touching two consecutive targets on the retina. The sclera contact forces are larger with higher variance while reorienting the eyeball, and remain relatively stable at a lower level while approaching the targets.

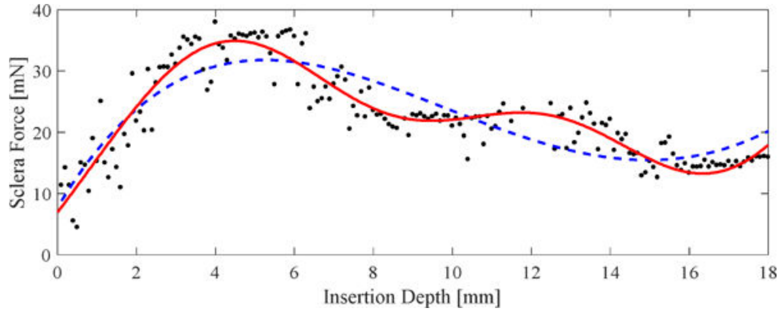

Figure 5.

A 4^{th} order polynomial fit (blue dashed) and a 3^{rd} order sum of sines regression (red solid) describing the median of measured sclera contact forces (black dotted) as a function of the tool insertion depth. The RMSE errors are 4.70 mN and 4.25 mN, respectively.